Charge transfer within clusters in liquid ionic alloys

1993 J. Phys.: Condens. Matter 5 4271

(http://iopscience.iop.org/0953-8984/5/26/002)

J. Phys.: Condens. Matter 5 (1993) 4271–4282. Printed in the UK

Charge transfer within clusters in liquid ionic alloys

Qiang Wang†, M P Iñiguez†, J A Alonso† and M Silbert‡

† Departamento de Fisica Teorica, Universidad de Valladolid, E-47011 Valladolid, Spain

‡ School of Physics, University of East Anglia, Norwich NR4 7TJ, UK

Received 15 January 1993

Abstract. Based on the Kohn–Sham equations of the density functional formalism and using the pseudopotential approximation, self-consistent calculations of the electron density distribution and structural stability in the Pb_4Na_4 and Pb_4Cs_4 clusters have been carried out. For the two clusters, the geometrical structures are similar: the Pb atoms are arranged in a regular tetrahedron inside, while the alkali metal atoms (Na or Cs) form a larger tetrahedron outside taking positions opposite to the faces of the Pb_4 unit. The charge transfer from the outer alkali metal atoms to the inner Pb_4 tetrahedron increases with decreasing electronegativity of the alkali metal atom. The net excess of charge in the Pb_4 unit is of the order of one electronic charge. We have used our results to discuss the liquid alloys $Pb_{0.5}Na_{0.5}$ and $Pb_{0.5}Cs_{0.5}$, where much higher charge transfer is normally assumed.

1. Introduction

An interesting class of equiatomic binary alloys is obtained by combining an alkali metal (Li, Na, K, Rb, Cs) with a tetravalent metal like Sn or Pb. As a consequence of the large difference in electronegativities one electron is normally assumed to be transferred from the alkali atom to Sn or Pb. The resulting anions (Sn^- or Pb^-) are isoelectronic with the P and As atoms, which in the gas phase form tetrahedral molecules P_4 and As_4. In a similar way the anions group together in the crystal forming Sn_4 and Pb_4 tetrahedra, assumed to be quadruply charged ($(Sn_4)^{4-}$, $(Pb_4)^{4-}$), similar to the so-called Zintl ions, separated by the alkali cations. Such tetrahedra have indeed been found in equiatomic solid alloys of Na, K, Rb and Cs with Sn and Pb, which are all isomorphic (Marsh and Shoemaker 1953, Hewaidy *et al* 1964, Müller and Volk 1977). The crystal structures in the solid can be described in terms of Pb_4 (or Sn_4) tetrahedra surrounded by larger, oppositely directed A_4 tetrahedra, where A indicates the alkali atom (Reijers *et al* 1989, Saboungi and Price 1992). The larger electronegativity of Li compared to the other alkali elements explains why the Li alloys are exceptions.

Considerable evidence exists for the survival of those tetrahedral Zintl ions in the liquid alloy after melting. First of all, the intermetallic alloy Cs–Pb becomes a plastic crystal, characterized by jump reorientations of Cs_4Pb_4 structural units, before melting (Saboungi and Price 1992). On the other hand, on plotting the resistivity of the liquid alloys as a function of concentration over the whole concentration range, a sharp maximum of the resistivity is observed at 50 at.% Pb in the alloys K–Pb, Rb–Pb, and Cs–Pb; for Li–Pb and Na–Pb the maximum occurs at 20 at.% Pb, although a small hump at 50 at.% Pb is also observed in Na–Pb. The shift of stoichiometry between Na–Pb and K–Pb is interpreted as a transition to tetrahedral Zintl ion formation in the alloy (van der Lugt 1991). The hump in Na–Pb at 50 at.% Pb suggests that only a fraction of the Pb atoms are in tetrahedral

0953-8984/93/264271+12$07.50

Zintl ion configurations. This transition has been confirmed by measurements of other physical properties like density, specific heat and, most illuminating of all, the stability function (van der Lugt 1991, Tumidajski *et al* 1990). Evidence for the existence of Zintl ions as geometrical units in the liquid has also been derived from structural measurements. A comprehensive neutron diffraction study of the equiatomic liquid alloys Na–Pb, K–Pb, Rb–Pb, Cs–Pb, K–Sn and Cs–Sn has been carried out (Reijers *et al* 1989, 1990). The interatomic Pb–Pb and Sn–Sn distances deduced from the radial distribution functions are equal to the Pb–Pb and Sn–Sn distances in the tetrahedra of the solid compounds. Molecular dynamics simulations in which the tetrahedra are explicitly used as geometrical units have been very successful in explaining the structural data except for those on Na–Pb (Reijers *et al* 1990). For this particular alloy the assumption that only a fraction of the Pb atoms are clustered while the rest are evenly distributed agrees better with the experiments.

The usual assumption of a complete transfer of one electron from each alkali atom to Sn or Pb seems rather questionable to us. It is difficult to imagine a stable cluster $(Sn_4)^{4-}$ or $(Pb_4)^{4-}$ with four excess electrons. The resistivity of the liquid $Pb_{0.5}Cs_{0.5}$ alloy is about twenty times that of $Pb_{0.5}Na_{0.5}$. This suggests quite a different metallic character, and a different degree of charge transfer. The measured conductivities in $Pb_{0.5}Na_{0.5}$ or $Pb_{0.5}K_{0.5}$ are hard to reconcile with the model of complete charge transfer. On the other hand we recognize that the number of external electrons in those clusters is twenty, which coincides with one of the magic numbers of simple metal clusters (Knight *et al* 1984). One could then justify the stability of $(Sn_4)^{4-}$ and $(Pb_4)^{4-}$ in part as a consequence of an electronic configuration of closed shells. To our knowledge the charge transfer in these alloys, and the electronic structure of the relevant clusters, has not been studied in detail, and this is our task in this paper. For this purpose we concentrate our attention on the representative clusters Pb_4Na_4 and Pb_4Cs_4. Although our calculations correspond to free, or gas phase, clusters we believe that our conclusions can be carried with little modification to the relevant case of liquid alloys.

2. Model

The high degree of short-range order in the liquid alloys of interest here suggests that the most salient features of the charge transfer in the alloy can be obtained from finite-cluster calculations. We use the density functional formalism (Kohn and Sham 1965, Parr and Yang 1989) to express the energy of the cluster (Hartree atomic units will be used through the paper unless explicitly stated):

$$E = T_s + \tfrac{1}{2}\int\int \rho(r)\rho(r')/|r-r'|\,\mathrm{d}^3r\,\mathrm{d}^3r' + \int \rho(r)V_I(r)\,\mathrm{d}^3r + E_{xc}[\rho] + \tfrac{1}{2}\sum_{i\neq j} U_{ij}. \quad (1)$$

In this expression T_s is the single-particle kinetic energy, the second term gives the classical coulomb interaction of the electronic cloud $\rho(r)$ with itself, the third term is the interaction between the electronic cloud and the external ionic background represented by a potential $V_I(r)$, $E_{xc}[\rho]$ is the exchange–correlation energy of the electrons, and the last term gives the sum of the ion–ion interactions. U_{ij} represents the interaction between ions at positions $\boldsymbol{R}_i$ and $\boldsymbol{R}_j$.

For a given geometry, characterized by the set $\{\boldsymbol{R}_j\}$ of atomic coordinates, the electron density is obtained by minimization of (1). This is achieved by solving the Schrödinger-like Kohn–Sham equations

$$\tfrac{1}{2}\nabla^2\Psi_i(r) + V_{\mathrm{eff}}(r)\Psi_i(r) = \epsilon_i\Psi_i(r) \quad (2)$$

and building the electron density from the occupied one-electron orbitals

$$\rho(\boldsymbol{r}) = \sum_{i}^{\text{occ}} |\Psi_i(\boldsymbol{r})|^2. \tag{3}$$

The effective potential of the Kohn–Sham equations is a sum of several contributions

$$V_{\text{eff}}(\boldsymbol{r}) = V_{\text{H}}(\boldsymbol{r}) + V_{\text{I}}(\boldsymbol{r}) + V_{\text{xc}}(\boldsymbol{r}) \tag{4}$$

where V_{H} is the electrostatic Hartree potential of the electronic cloud:

$$V_{\text{H}}(\boldsymbol{r}) = \int \rho(\boldsymbol{r}')/|\boldsymbol{r} - \boldsymbol{r}'|\, \mathrm{d}^3\boldsymbol{r}'.$$

V_{I} is the external potential of the ionic skeleton

$$V_{\text{I}}(\boldsymbol{r}) = \sum_{j} v(|\boldsymbol{r} - \boldsymbol{R}_j|) \tag{5}$$

and $V_{\text{xc}}(\boldsymbol{r}) = \delta E_{\text{xc}}[\rho]/\delta\rho(\boldsymbol{r})$ is the exchange–correlation potential. The local density approximation (LDA) will be used for exchange and correlation effects. In particular we employ the LDA functional of Gunnarsson and Lundqvist (1976). On the other hand the pseudopotential $v(|\boldsymbol{r} - \boldsymbol{R}_j|)$ of the ion at position $\boldsymbol{R}_j$ is modelled with the empty core pseudopotential (Ashcroft 1966), which is zero inside the core of radius r_{c} and purely coulombic outside. For the atoms of interest we take the following values of the core radius: $r_{\text{c}}(\text{Na}) = 1.74$ au, $r_{\text{c}}(\text{Cs}) = 2.74$ au, $r_{\text{c}}(\text{Pb}) = 1.20$ au. For the monovalent atoms Na and Cs, r_{c} was obtained by fitting to experiment the first ionization potential obtained in a density functional pseudopotential calculation. In the case of Pb the quantity fitted was the sum of the first, second, third and fourth ionization potentials.

For a general cluster the solution of the Kohn–Sham equations is complicated by the multi-centre nature of the problem. Furthermore, if we are interested in calculating the equilibrium geometry of the cluster (this is the case as we will see immediately below), then the Kohn–Sham equations have to be solved many times, that is for many cluster configurations, during the process of searching for the lowest energy geometry. For this reason we make the approximation of replacing $V_{\text{I}}(\boldsymbol{r})$ of (5) by its spherical average $V_{\text{I}}^{\text{av}}(\boldsymbol{r})$ about the centre of the cluster. In this way we only keep the spherically symmetric component of the electron–ion background interaction (Iñiguez *et al* 1989). In spite of this approximation, the ion–ion interaction term of (1) is calculated without approximation, that is, taking full account of the cluster geometry.

For calculating the equilibrium configuration the energy of the cluster also has to be minimized with respect to the set of atomic positions $\{\boldsymbol{R}_j\}$. This minimization has been performed using steepest-descent methods. An initial arbitrary geometry is first generated and the Kohn–Sham equations are solved to calculate the density, the energy and the forces on all the ions. Since the forces are very unlikely to be zero (that is, the cluster is not at equilibrium), then each ion is assigned a small displacement in the direction of the net force acting on it. For the new geometry the Kohn–Sham equations are again integrated and the forces recalculated. This process is iterated until the forces on all ions are zero, that is, until the cluster is at equilibrium. By this procedure the cluster can end up trapped in a metastable minimum different from the absolute energy minimum. To avoid this possibility the whole process is repeated a number of times, each time starting with a different initial geometry. Since our clusters are small, this procedure of searching for the equilibrium geometry is comprehensive enough. However, large clusters need a more sophisticated strategy like simulated annealing (Borstel *et al* 1992).

3. Results

3.1. Equilibrium geometry

Applying the steepest-descent strategy discussed in section 2 we have calculated the equilibrium structure of the clusters Na_4Pb_4 and Cs_4Pb_4. The most stable geometry, plotted in figure 1, can in both cases be described as an inner core formed by the four Pb atoms in a tetrahedral arrangement, surrounded by an external shell formed by the four alkali atoms, also forming a tetrahedral arrangement in such a way that each alkali atom is on top of one of the faces of the Pb tetrahedron. This structure has also been proposed for the cluster K_4Sb_4 by Hagelberg *et al* (1992). It is gratifying to find out that our calculations predict the tetrahedral clustering of Pb atoms found in the solid PbA alloys (the Pb_4 tetrahedron is a little distorted in the crystal) and proposed to occur also in the liquid alloys (van der Lugt 1991). Of course, A indicates the alkali element. Furthermore, the closest environment surrounding the Pb_4 tetrahedron in the crystal is formed by eight alkali atoms, four of them forming a tetrahedron oppositely directed (Reijers *et al* 1989) just as we predict from our cluster calculations. The Pb_4Cs_4 units persist in the newly discovered plastic crystal phase of the alloy Pb–Cs (Saboungi and Price 1992). This phase occurs in a narrow range of temperature before melting of the intermetallic compound. The new phase is characterized by jump reorientations of the Pb_4Cs_4 units.

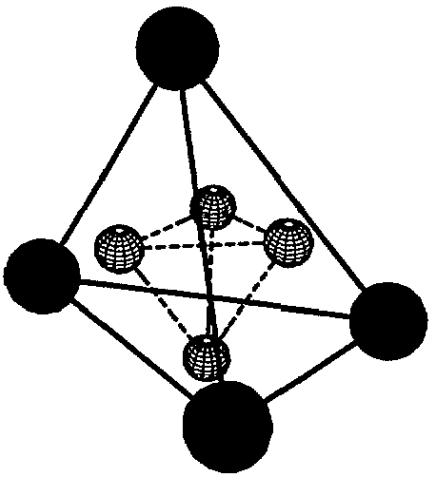

Figure 1. Calculated equilibrium structure of Pb_4A_4, where A is an alkali metal atom.

Our results justify the models used by Reijers *et al* (1989) in the analysis of the structural data of the liquid alloys obtained by neutron diffraction experiments. These authors used the random packing of structural units (RPSU) model and the reference interaction site model (RISM). In both models the structural unit was the Pb_4A_4 cluster formed by the Pb_4 tetrahedron surrounded by a larger A_4 tetrahedron oppositely directed.

The calculated interatomic distances are given in table 1. We give the Pb–Pb, Na–Na and nearest Na–Pb distances, as well as the distances from the Pb and Na atoms to the centre of the cluster. Comparing with experimental results obtained from structural measurements for the equiatomic liquid alloys (Reijers *et al* 1989)—the numbers given in table 1 actually correspond to the first two maxima in the radial distribution function—we find that our Pb–Pb distances are smaller for both systems. On the other hand the calculated Cs–Pb distance is larger and the calculated Na–Pb distance is smaller than the experimental values.

The interpretation of the differences is that, in the liquid Cs–Pb alloy the Pb_4 tetrahedra are larger than the corresponding tetrahedra in our model clusters, and that the Cs atoms are closer to the faces of Pb_4 than in our model cluster. These two differences tend to cancel each other and the resultant size of the Pb_4Cs_4 clusters should not be very different from our prediction. Incidentally, we recall here the well known tendency of the LDA to underestimate interatomic distances. This can account for our underestimation of the size of the Pb–Pb distances. We also note that our Cs–Pb distance (7.69 au) is very close to the experimental Cs–Pb distance in the crystal: 7.73 au (Reijers *et al* 1989).

Table 1. Interatomic distances (in au). CM indicates the centre of mass of the cluster.

Pb_4Na_4	Pb–Pb	Na–Pb	Na–Na	Pb–CM	Na–CM
Cluster	4.86	6.10	10.45	2.98	6.43
Others (MD)[a]	5.90	6.12	—	3.55	6.46
Experiment[b] (Liquid)	6.18	6.99	—	—	—
Pb_4Cs_4	Pb–Pb	Cs–Pb	Cs–Cs	Pb–CM	Cs–CM
Cluster	4.84	7.69	13.25	2.97	8.15
Others (MD) [a]	5.84	7.43	—	3.57	8.51
Experiment [b] (Liquid)	5.95	7.09	—	—	—

[a] Molecular dynamics simulations of Reijers *et al* (1990).
[b] Reijers *et al* (1989).

The comparison for the Na–Pb system is more difficult. As we have indicated in the introduction, Pb_4 clustering is only partial in this alloy, and Na_4Pb clustering, with the four Na atoms surrounding the Pb atom, also appears to be likely (van der Lugt 1991). Consequently, a comparison of our interatomic distances to measured ones (which are really averages over all the local configurations present in the alloy) is less justified in this case. Since interatomic distances have been measured in solid NaPb and in this case the existence of the tetrahedral units is confirmed (Reijers *et al* 1989) we can compare the data to our calculated interatomic distances: (i) again we find that the measured Pb–Pb distances are larger than the calculated ones, (ii) the Na–Pb distances in the solid (6.71 au) compare better with our cluster case than the Na–Pb distances deduced from measurements in the liquid alloy, and (iii) the fact that the Pb–Pb distances are predicted to be nearly independent of the other component is the same trend found for the Pb–Pb distances in the crystals. In table 1 we have also included interatomic distances obtained from the molecular dynamics simulations of Reijers *et al* (1990) for liquid Na–Pb and Cs–Pb alloys. In the simulations the alloy was considered as a mixture of A^+ and $(Pb_4)^{4-}$ ions. The pair potential between particles i and j, if they are not Pb^- ions belonging to the same tetrahedron, was a Born–Mayer–Huggins-type potential whereas the Pb–Pb interactions within $(Pb_4)^{4-}$ were approximated by a harmonic potential. The parameters of those potentials were chosen such that the simulations yielded a reasonable description of the structure factors obtained from neutron diffraction experiments. The Pb–Pb and Na–Pb interatomic distances obtained from the simulation (actually from the first maximum of the partial pair-correlation functions) lie midway between our cluster results and the experimental results already discussed.

Apart from the LDA approximation for exchange and correlation effects, other approximations which affect the calculated interatomic distances are, first of all, the spherical averaging of the cluster ionic pseudopotential and second, the fact that we are modelling

free clusters. It is well established that interatomic distances in small gas phase metallic clusters are a little contracted with respect to the same metal in the bulk phase.

3.2. Electronic distribution and charge transfer

The electron density distribution of the clusters Pb_4Na_4 and Pb_4Cs_4, corresponding to the calculated equilibrium geometries, have been plotted in figures 2(*a*) and 2(*b*) respectively (solid lines). On the other hand, the energies of the Kohn–Sham electronic shells have been plotted in figure 3 for the same clusters. The electronic configuration is, in both cases, $1s^21p^62s^21d^{10}$. This means that the clusters have the electronic configuration of closed shells, which evidently gives a large stability; also note that 20 is an electronic magic number for simple metal clusters (Knight *et al* 1984). Also in figure 3 we have plotted the electronic configurations of the non-interacting fragments Pb_4 and Na_4 (or Cs_4), in which we have arbitrarily fragmented the clusters. Consideration of these fragments will help us in the analysis of charge transfer effects. To be more precise, we have first considered an isolated neutral Pb_4 cluster having the same structure and interatomic distances as the Pb_4 tetrahedron in Pb_4Na_4 (or Pb_4Cs_4). Incidentally we mention that the equilibrium structure of free Pb_4 in our model is also the tetrahedron. We have then calculated the electronic structure of the neutral Pb_4 unit. The electronic configuration we have found is $1s^21p^62s^21d^6$. The energy eigenvalues corresponding to those shells have been plotted in figure 3, and the electron density of the Pb_4 unit is given in figure 4. For the other fragment, Na_4 or Cs_4, we have followed a similar approach. We have first modelled a Na_4 (or Cs_4) fragment as a tetrahedron with the same interatomic distances that Na_4 or Cs_4 have in Pb_4Na_4 and Pb_4Cs_4, and we have calculated the electronic structure of those alkaline fragments. The results have been plotted in figure 3 and the corresponding electron density in figure 4. The density of the Pb_4 fragment has a peak at 4 au and a shoulder to the left hand side; the Na_4 density is more extended, having a broad peak centred at 7 au (at 9 au for Cs_4); we notice from table 1 that the Na and Cs atoms are at 6.43 au and 8.15 au from the cluster centre respectively. Comparing the energy level structure of the Pb_4A_4 cluster and those of the non-interacting neutral fragments Pb_4 and A_4 it is tempting to conclude that the alkali fragment loses its four electrons, which go to fill the highest occupied shell (1d) of Pb_4. This interpretation would seem to agree with the standard view (van der Lugt 1991), but we also appreciate that, as a consequence of the charge transfer towards Pb_4, the electronic levels have been shifted to lower binding energies by a sizeable amount. Due to this shift the 1d shell has a binding energy close to the binding energies of the occupied levels in the neutral Na_4 (or Cs_4) model fragments (this is especially true for Pb_4Cs_4). This indicates that the 1d wavefunctions in Pb_4A_4 have a sizeable amplitude over the external part of the cluster, which is the region we associate with the alkali atoms. In summary, we think that the interpretation of the results in the energy level diagrams of figure 3 as a full charge transfer leading to formation of $(Pb_4)^{4-}$ is not justified. Now we substantiate our claim by performing a careful analysis of the charge transfer effect based on the analysis of the charge redistribution and on the variation of the energy levels of Pb_4 by charging the Pb_4 unit.

Subsequently, starting from the electron densities of the non-interacting Pb_4 and Na_4 (or Cs_4) pieces, given in figure 4, and adding these we have constructed the total electron density of the non-interacting Pb_4Na_4 and Pb_4Cs_4 clusters. Those non-interacting densities are represented by the broken curves in figure 2. Comparing these with the interacting densities (solid curves in figure 2), we appreciate in the interacting densities a depletion of the electronic density on the outer part of the clusters (this is the region occupied by the alkali atoms) and an important accumulation of extra charge in the region occupied by

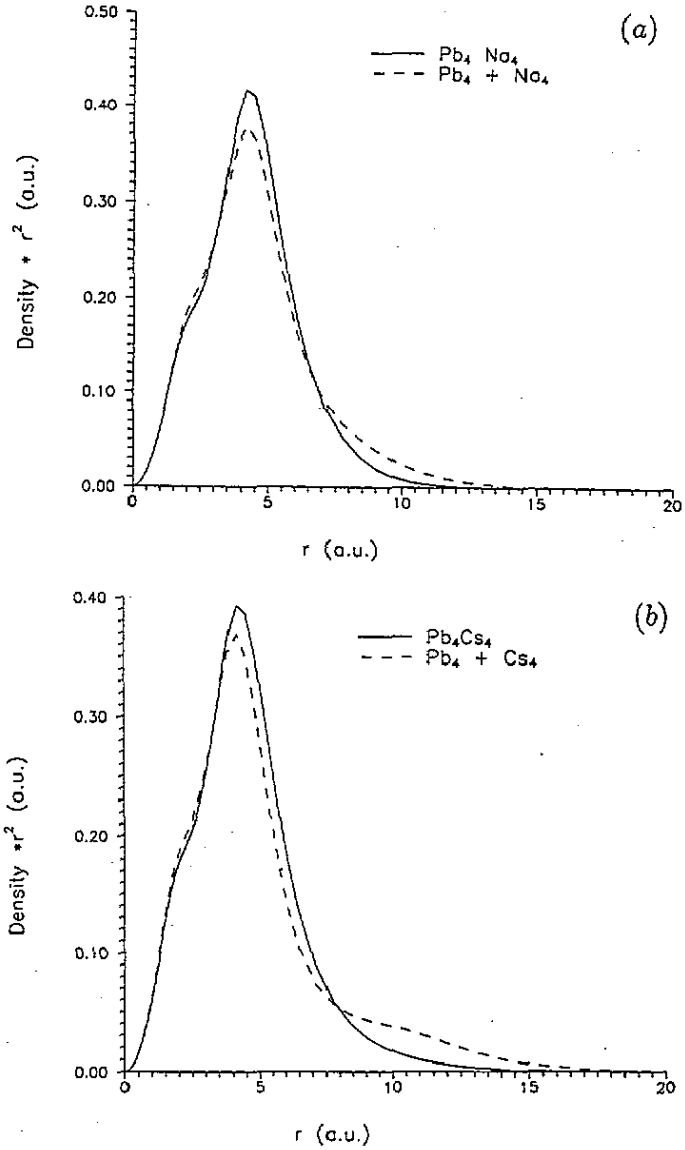

Figure 2. Electron density of (*a*) Na_4Pb_4 and (*b*) Cs_4Pb_4 for the geometry of minimum energy (solid curves). An electron density is also plotted (broken curves), obtained from non-interacting Pb_4 and Na_4 (or Cs_4) fragments (see text).

the Pb atoms. This is a consequence of the interaction between the fragments, that is, a consequence of the self-consistency of the calculation. This observation agrees with the expected charge transfer towards Pb_4 due to the larger electronegativity of the Pb atoms.

The flow of charge from the outer to the inner part of the cluster is better appreciated in figure 5, where we have plotted

$$\Delta\rho(r) = \rho(r) - \rho_{ni}(r) \tag{6}$$

where $\rho(r)$ is the contribution from the self-consistent calculation for the cluster and $\rho_{ni}(r)$ is the density constructed from the two non-interacting fragments. $\Delta\rho$ is negative in the outermost part of the cluster. This feature is associated to the 1s and 1p electrons of the alkali fragment (see figures 2 and 3) which, in the interacting cluster, become part of the 1d

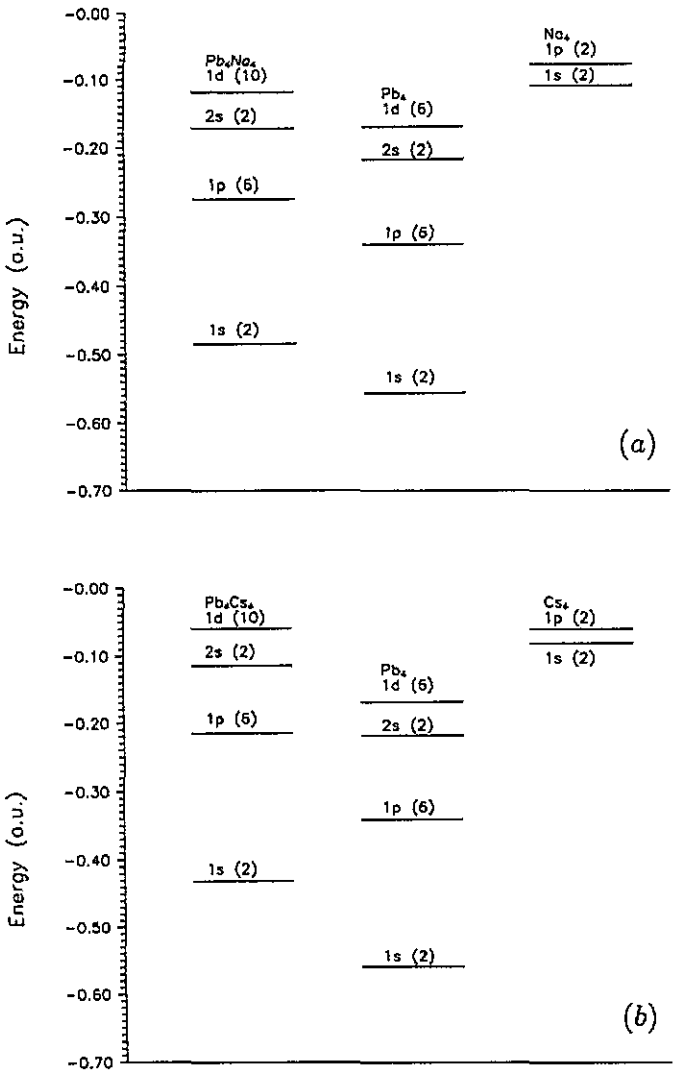

Figure 3. (*a*) Kohn–Sham energy eigenvalues for the cluster Pb_4Na_4 and for the two separated neutral fragments Pb_4 and Na_4. The geometric structure of those fragments is the same as in the compound cluster. The occupation of the electronic shells is given in brackets. (*b*) Analogous data for Pb_4Cs_4.

shell, which is, however, more diffuse than the 1d shell in the non-interacting Pb_4 fragment. A reasonable quantitative measure of the charge transfer ΔQ can be given by the integral

$$\Delta Q = 4\pi \int_{r_0}^{\infty} (\rho(r) - \rho_{ni}(r)) r^2 \, dr \tag{7}$$

where the lower limit r_0 is indicated in the figure. This gives values 0.95 and 1.38 for the charge transfer in Pb_4Na_4 and Pb_4Cs_4 respectively.

The other region of negative values of $\Delta\rho(r)$, around 2–3 au, is not due to direct charge transfer from Na to Pb. Instead it can be viewed as an indirect effect due to charge transfer. Direct charge transfer induces a shift of the electronic levels to lower binding energies because of the enhanced screening of the Pb_4 pseudopotential due to the transferred charge. The lower binding energy then pushes the electrons (especially the innermost ones) away from the innermost part of the cluster, and this is precisely the effect observed.

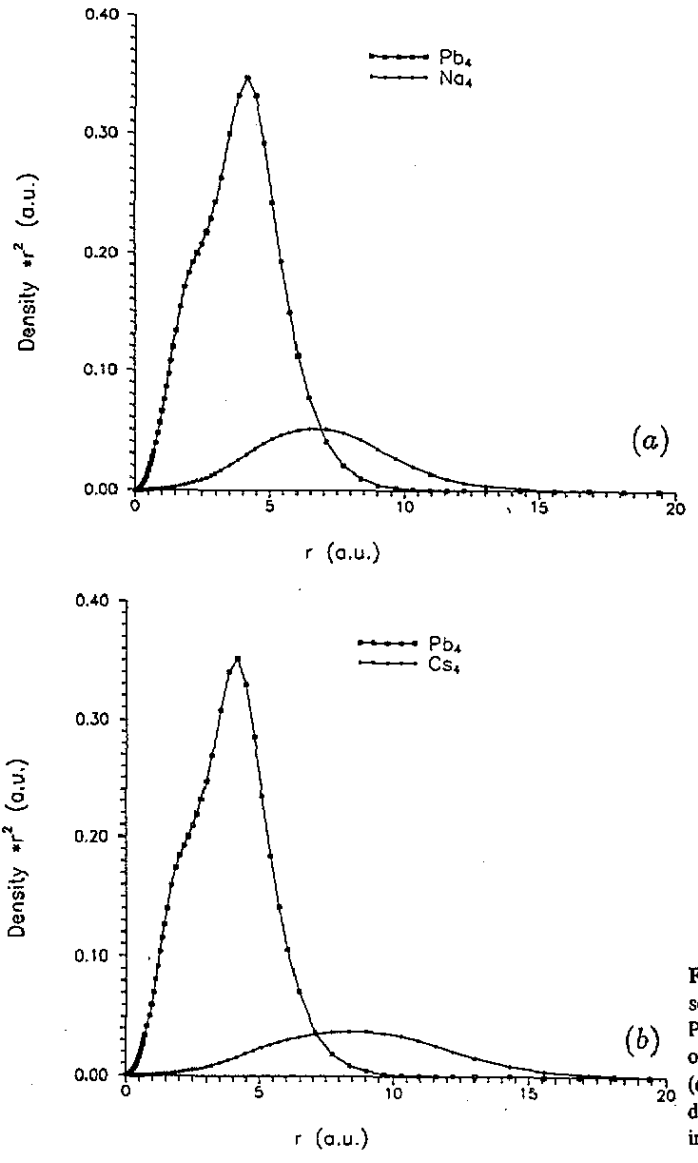

Figure 4. Electron density of the separated non-interacting fragments Pb_4 and Na_4 (or Cs_4) at the geometry of the real cluster Pb_4Na_4 (or Pb_4Cs_4). Adding these fragment densities leads to the broken curves in figure 2.

In summary we propose that the charge transfer in Pb_4Na_4 *and* Pb_4Cs_4 *is in the range* 1–1.5*e*, that is, smaller than normally assumed. Since this conclusion is in conflict with the naive interpretation based on the filling of the electronic levels (see figure 2) we give now further support to our proposal using an argument based on the shift of the electron energy eigenvalues induced by the charge transfer. In figure 6 we show the results of two self-consistent calculations for the isolated Pb_4 fragment. The first calculation is for neutral Pb_4 and the second calculation for the negative singly charged fragment, that is $(Pb_4)^-$. In both cases the geometric structure is the tetrahedron, and the interatomic distances are assumed to be independent of the charge state. The shifts of the energy eigenvalues of the different shells are large and nearly constant. Actually, the shifts induced by the extra electron placed on Pb_4 are larger than the shifts obtained when Pb_4 combines with the four

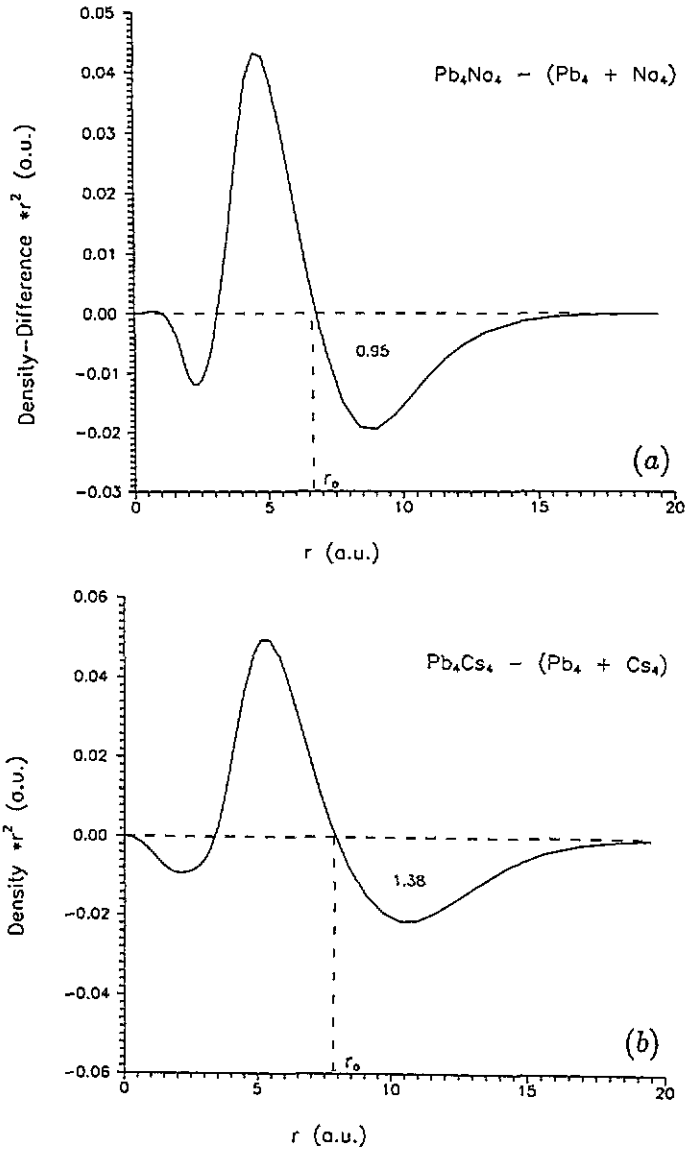

Figure 5. Electron density difference $\rho(r) - \rho_{ni}(r)$ between the self-consistent and non-interacting densities of figure 2. The charge transfer to the Pb_4 unit is the number attached to the curve.

alkali atoms to form Pb_4A_4. Evidently free Pb_4^- is not the same as charged Pb_4 in Pb_4A_4, but our results suggest that the shifts we observe in Pb_4A_4 are only consistent with a total charge transfer from A_4 to Pb_4 of the order of one electron, which is also the figure obtained from the analysis of the electron density distribution.

One aspect of our calculation that could slightly affect the amount of charge transfer is that the interatomic distances we have used in the calculation differ a little from the experimental ones. To avoid any reservations arising from this point we have repeated all our self-consistent calculations using the experimental interatomic distances given in table 1. This means that the energy eigenvalues, wavefunctions and electron densities have been recalculated for the experimental interatomic distances. The conclusions are essentially the same, although there are a few differences of detail on which we now comment.

As a consequence of the small expansion of the Pb_4A_4 clusters (especially the Pb_4 unit)

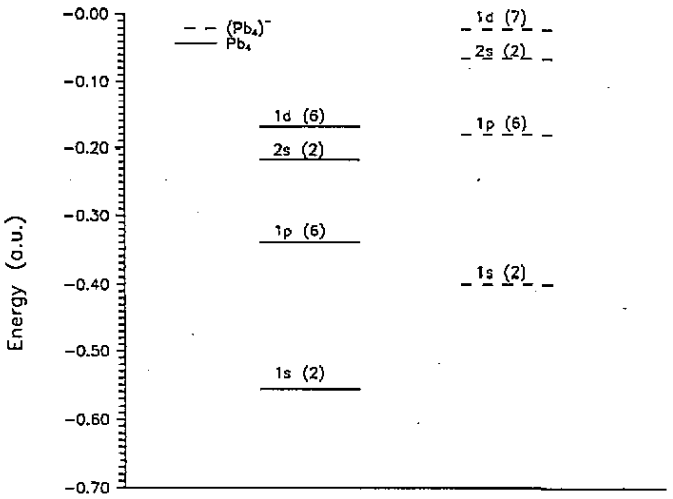

Figure 6. Energy eigenvalues for Pb_4 and $(Pb_4)^-$ with the tetrahedral structure and identical interatomic distances. Occupation numbers are given in brackets.

the binding energies of the 1s, 1p, and 2s shells decrease a little, whereas the binding of the 1d shell increases. Although the ordering of the shells is still 1s, 1p, 2s, 1d, and the electronic configuration is one with closed shells, the 2s and 1d shells are now very close in energy. A similar situation occurs for the Pb_4 fragment. In this case the 1s, 1p and 2s levels also become less tightly bound in the expanded fragment, whereas the 1d level has a binding energy similar to that in the more compressed case. Again the 2s and 1d shells become very close in energy. The charge transfer, defined from the difference of electron densities as in (7), is now $0.82e$ for Pb_4Na_4 and $1.07e$ for Pb_4Cs_4. These values are compared with the previous charge transfer values in table 2, where we observe that the charge transfer decreases only slightly as a consequence of the cluster expansion, leaving our conclusions unaffected.

Table 2. Interatomic distances (in au) and charge transfer (according to (7)) in Pb_4Na_4 and Pb_4Cs_4. I: distances from the theoretical equilibrium geometry. II: experimental distances from liquid alloy data (Reijers *et al* 1989).

Pb_4Na_4	Pb–Pb	Pb–Na	ΔQ_e	Pb_4Cs_4	Pb–Pb	Pb–Cs	ΔQ_e
I	4.86	6.10	0.95	I	4.83	7.69	1.38
II	6.18	6.99	0.82	II	5.95	7.09	1.07

4. Summary and comments

In conclusion we have found that the usual assumption of a full transfer of four electrons to Pb_4 to form $(Pb_4)^{4-}$ in liquid PbA alloys (A is an alkali element) seems an overestimate. Although, according to our density functional calculations, the clusters Pb_4Na_4 and Pb_4Cs_4 have closed electronic shells and therefore have a certain similarity to the magic clusters with 20 electrons in typical metallic materials, our analysis, based on (i) charge density difference plots, and (ii) the study of the shift of the shell-energy eigenvalues as the Pb_4 unit takes up electronic charge, indicates that the amount of charge that Pb_4 is able to take up in these alloys is not much more than one electron.

There are several options to improve the quality of our calculations, although we expect that the conclusions will remain basically the same. One is to take some account of the environment around the Pb_4A_4 cluster in the liquid. This would require changing the boundary conditions in the process of solving the Kohn–Sham equations and could be achieved by embedding the cluster in an effective medium. To this end the cluster could be assigned an effective volume equal to the experimental volume per Pb_4A_4 unit in the liquid. This will remove some of the inaccuracies in the interatomic distances, although our model calculations already indicate clearly (see table 2) that the errors in the interatomic distances affect the charge transfer only in a minor way.

More importantly, one could avoid the approximation of a spherically symmetric electron–ion background interaction. In this case an accurate ionic pseudopotential (ideally, a non-local pseudopotential) could be used. This fully three-dimensional calculation is in our present plans.

Acknowledgments

This work has been supported by DGICYT (grant PB 89-0352) and by the Science Program of the European Community (project SC1*-CT91-0754). One of us (QW) acknowledges a postdoctoral grant from Ministerio de Educacion y Ciencia of Spain.

References

Ashcroft N W 1966 *Phys. Lett.* **23** 48

Borstel G, Lammers U, Mañanes A and Alonso J A 1992 *Nuclear Physics Concepts in Atomic Cluster Physics* ed R Schmidt, H O Lutz and R Dreizler (Berlin: Springer) p 327

Gunnarsson O and Lundqvist B I 1976 *Phys. Rev.* B **13** 4274

Hewaidy I F, Busmann E and Klem W 1964 *Z. Anorg. Allg. Chem.* **328** 283

Hagelberg F, Neeser S, Sahoo N, Das T P and Weil K G 1992 *Physics and Chemistry of Finite Systems: From Clusters to Crystals* vol I, ed P Jena, S N Khanna and B K Rao (Dordrecht: Kluwer) p 593

Iñiguez M P, Lopez M J, Alonso J A and Soler J M 1989 *Z. Phys.* D **11** 163

Knight W D, Clemenger K, de Heer W A, Saunders W A, Chou M Y and Cohen M L 1984 *Phys. Rev. Lett.* **52** 2141

Kohn W and Sham L J 1965 *Phys. Rev.* A **140** 1133

Marsh R E and Shoemaker D P 1953 *Acta Crystallogr.* **6** 197

Müller W and Volk K 1977 *Z. Naturf.* b **32** 709

Parr R G and Yang W 1989 *Density Functional Theory of Atoms and Molecules* (New York: Oxford University Press)

Reijers H T J, Saboungi M L, Price D L, Richardson J W, Volin K J and van der Lugt W 1989 *Phys. Rev.* B **40** 6018

Reijers H T J, Saboungi M L, Price D L and van der Lugt W 1990 *Phys. Rev.* B **41** 5661

Reijers H T J, van der Lugt W and Saboungi M L 1990 *Phys. Rev.* B **42** 3395

Saboungi M L and Price D L 1992 *J. Non-Cryst. Solids* **150** 260

Tumidajski P J, Petric A, Takenaka T, Pelton M and Saboungi M L 1990 *J. Phys.: Condens. Matter* **2** 209

van der Lugt W 1991 *Phys. Scr.* T **39** 372